$Tl_1Ca_{n-1}Ba_2Cu_nO_{2n+3}$ ($n = 1,2,3$): A New Class of Crystal Structures Exhibiting Volume Superconductivity at up to $\simeq 110$ K

S. S. P. Parkin, V. Y. Lee, A. I. Nazzal, R. Savoy, and R. Beyers

IBM Almaden Research Center, San Jose, California 95120

and

S. J. La Placa

IBM Thomas J. Watson Research Center, Yorktown Heights, New York 10598

We report the discovery of three new phases in the Tl-Ca-Ba-Cu-O system, $Tl_1Ca_{n-1}Ba_2Cu_nO_{2n+3}$ ($n = 1,2,3$), one of which ($n = 3$) exhibits bulk superconductivity at $\simeq 110$ K. The crystal structures of these new materials are closely related to that of $Tl_2Ca_2Ba_2Cu_3O_x$, the recently discovered 125-K superconductor. All of these compounds contain Cu perovskitelike units, but whereas these are separated by bilayer Tl-O sheets in the 125-K material, they are separated by *monolayer* Tl-O sheets in the new structures, enabling an examination of the effect of the coupling between successive Cu perovskite units on superconducting properties.

PACS numbers: 74.70.Vy

A number of high-temperature superconducting compounds have recently been discovered in the Bi-Ca-Sr-Cu-O [1-9] and Tl-Ca-Ba-Cu-O [10-13] systems, with bulk superconductivity found at 125 K in $Tl_2Ca_2Ba_2Cu_3O_{10\pm y}$.[12] Three related crystal structures have been reported in these systems, all containing either Bi-O or Tl-O bilayers that separate Cu perovskitelike units. The structural differences in the superconducting phases identified thus far—$Bi_2Sr_2Cu_1O_{6\pm y}$, $Bi_2Ca_1Sr_2Cu_2O_{8\pm y}$, $Tl_2Ba_2Cu_1O_{6\pm y}$, $Tl_2Ca_1Ba_2Cu_2O_{8\pm y}$ ("2122"), and $Tl_2Ca_2Ba_2Cu_3O_{10\pm y}$ ("2223")—lie in the number of Cu layers in the perovskite unit. The empirical observation that the superconducting transition temperature, T_c, increases with increased size of the Cu perovskite unit seems to confirm longstanding speculations in this regard. The role of the layers that separate the Cu perovskite units is less certain. Herein, we report the discovery of a new class of crystal structures comprising three phases of the form $Tl_1Ca_{n-1}Ba_2Cu_nO_{2n+3}$ ($n = 1,2,3$), which contain monolayer, bilayer, or trilayer Cu perovskitelike units separated by *monolayer* Tl-O sheets.

The samples were prepared by our thoroughly mixing Tl_2O_3, CaO, BaO_2, and CuO powders. After grinding, the mixtures were pressed into pellets and wrapped in gold. The pellets were fired at 880°C for 3 h in a sealed quartz tube containing approximately 1 atm oxygen, then furnace cooled to room temperature over a 4-h period. In this Letter the preparation and properties of the $Tl_1Ca_2Ba_2Cu_3O_{9\pm y}$ phase—hereafter referred to as "1223"—are described in some detail. Similarly comprehensive studies of the related compounds $Tl_1Ba_2Cu_1O_{5\pm y}$ ("1021") and $Tl_1Ca_1Ba_2Cu_2O_{7\pm y}$ ("1122") will be described elsewhere.

Figure 1 shows resistance versus temperature curves for two samples, A and B, of starting composition $Tl_{0.85}Ca_2Ba_2Cu_3$ prepared under nominally the same conditions. Data for samples containing primarily the $Tl_2Ca_1Ba_2Cu_2O_{8\pm y}$ and $Tl_2Ca_2Ba_2Cu_3O_{10\pm y}$ phases are shown for comparison. Thus far, we have found that a starting metal-cation composition deficient in thallium —$Tl_{0.85}Ca_2Ba_2Cu_3$—gives the largest percentage of the $Tl_1Ca_2Ba_2Cu_3O_{9\pm y}$ phase. Starting exactly at the $Tl_1Ca_2Ba_2Cu_3$ composition gives $Tl_2Ca_2Ba_2Cu_3O_{10\pm y}$ as the predominant superconducting phase.[12] The resis-
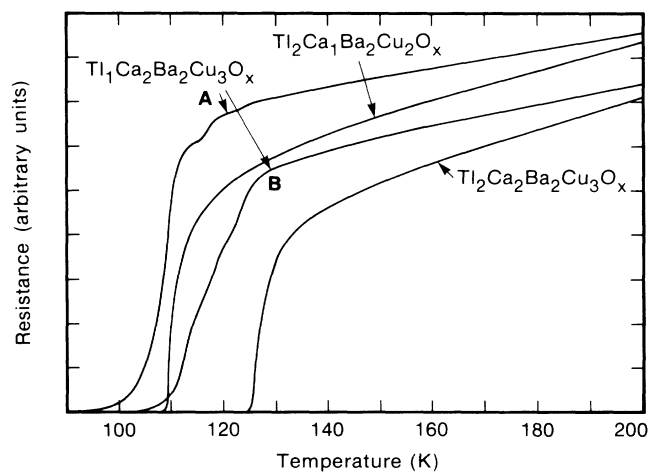

FIG. 1. Resistance vs temperature curves for two samples of nominal composition $Tl_{0.85}Ca_2Ba_2Cu_3O_{9\pm y}$. Data for material containing predominantly $Tl_2Ca_2Ba_2Cu_3O_{10\pm y}$ and $Tl_2Ca_1Ba_2Cu_2O_{8\pm y}$ are included for comparison. The curves have been arbitrarily scaled so that they do not overlap in the figure.

tance measurements were made with a standard low-frequency lock-in method with four probes and platinum or silver paint contacts. Figure 2 shows magnetic susceptibility versus temperature plots for the same four samples, measured with a S.H.E. (B.T.I.) Corp. dc SQUID magnetometer. These data were taken by our cooling the samples in a field of 100 Oe. The resistivity and Meissner data are in good agreement with one another. The 2122 and 2223 phases have transition temperatures of $\simeq 108$ and 125 K, respectively.[12] Both samples A and B contain minor components that become superconducting near 125 and 118 K but there is a larger amount for sample B. The bulk of sample A becomes superconducting just below 110 K and that of sample B just above 110 K. Since the samples are multiphase, there is some uncertainty in the determination of T_c for $Tl_1Ca_2Ba_2Cu_3O_{9 \pm y}$. On the basis of our microstructural analysis (see below), we believe that it is reasonable to assign T_c to the temperature at which the major portion of samples A and B become superconducting ($\simeq 110$ K). Since the Meissner data indicate superconducting fractions ($\simeq 10\%$–20%) in the $Tl_{0.85}Ca_2Ba_2Cu_3O_x$ samples comparable to those found in typical 2122 samples, yet x-ray and microprobe data indicate only small amounts of 2122 and 2223 material in samples A and B, we are confident of this assignment.

The microstructures of the two $Tl_{0.85}Ca_2Ba_2Cu_3$ samples were examined by electron microprobe analysis, x-ray powder diffractometry, and transmission electron microscopy. While all three techniques showed the samples comprised several phases, electron microprobe analysis found the composition of the predominant phase
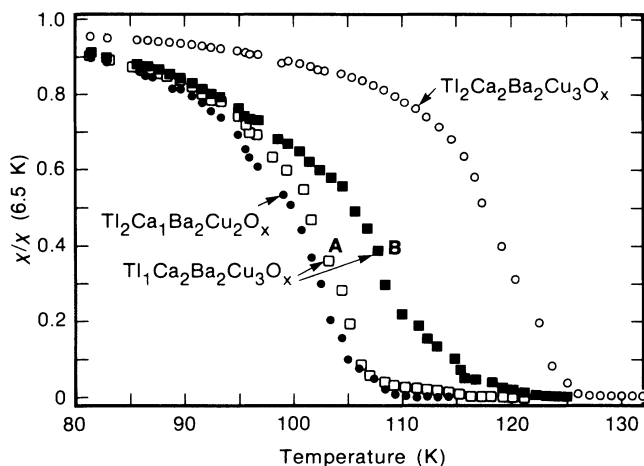

FIG. 2. Meissner susceptibility (normalized to 1 at 6.5 K) vs temperature for two samples of nominal composition $Tl_{0.85}Ca_2Ba_2Cu_3O_{9 \pm y}$ (A, open squares; B, filled squares). Data for materials composed predominantly of $Tl_2Ca_2Ba_2Cu_3O_{10 \pm y}$ (open circles) and $Tl_2Ca_1Ba_2Cu_2O_{8 \pm y}$ (filled circles) are also shown. All curves were measured in an applied field of 100 Oe.

($\gtrsim 60\%$) in these samples to be almost identical, namely, $Tl_{1.06}Ca_{1.82}Ba_{2.00}Cu_{2.99}$ and $Tl_{1.05}Ca_{1.83}Ba_{2.00}Cu_{3.06}$ for samples A and B, respectively. Microprobe analysis also identified $BaCuO_2$, a phase of approximate composition $Tl_1Ca_{10}Cu_{13}O_x$, as well as trace amounts ($<5\%$) of $Tl_2Ca_1Ba_2Cu_2O_{8 \pm y}$. The presence of $BaCuO_2$ is consistent with a large Curie contribution found in the normal-state magnetic susceptibility. The microstructure of sample B was quite different from that of sample A. In particular the crystallites of the 1223 phase ($\simeq 10$–20 μm in extent) contained narrow bands, $\simeq 1$ μm wide, with a significantly enriched Tl content. Their average composition was analyzed to be $Tl_{1.24}Ca_{1.76}Ba_{2.00}Cu_{3.01}$.

The structure of sample A was determined from its x-ray powder diffraction pattern. Almost all of the lines in the pattern could be indexed to a primitive tetragonal cell with dimensions $a = 3.8429(6)$ and $c = 15.871(3)$ Å. This cell was confirmed by electron diffraction studies (Fig. 3), which also indicated that there is a weak superlattice with an approximate wave vector [0.29, 0, 0.5] in this material. The superlattice was too weak to be observed in the x-ray data and is neglected in the following structural analysis. The intensities of the remaining lines could be indexed to the 2122 unit cell and indicated that about 6% of this phase was present relative to the primary 1223 phase, consistent with the microprobe data. Microprobe and x-ray powder diffraction data showed that sample B contains a slightly larger amount of the 2122 phase. No evidence for the 2223 phase was found from these analyses in either sample A or B.

The Cu-$K\alpha$ powder intensity data were collected on a 2-kW Philips diffractometer with use of a (002) pyrolytic-graphite post-beam monochromator and a $0.05°$ 2θ step-scan mode. After background subtraction, peak height intensities—corrected for low-angle sample illumination, multiplicity, and Lorentz polarization effects—were taken as observed structure factors. Conventional Patterson and Fourier methods were used to
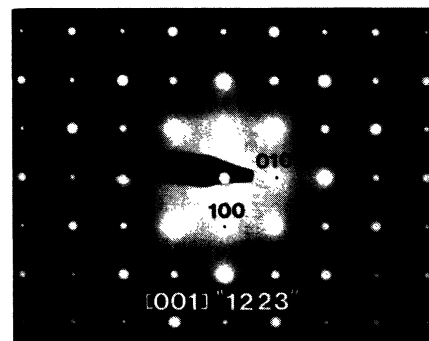

FIG. 3. Selected-area transmission-electron-microscopy diffraction pattern along the [001] axis that confirms the primitive tetragonal cell and also indicates the presence of a weak superlattice.

determine the preliminary heavy-atom structure of $Tl_1Ba_2Ca_2Cu_3O_{9\pm y}$. Despite problems of peak overlap, sample texture, and the inherent limitations of x-ray powder data, these methods have been demonstrated to be effective in this class of materials, which have tetragonal or pseudotetragonal symmetry and two short axes (≈ 3.8 Å).[7] The metal atoms are thus forced to occupy $0,0,z$ or $\frac{1}{2},\frac{1}{2},z$ sites.

Table I summarizes the calculated positional parameters for $Tl_1Ca_2Ba_2Cu_3O_{9\pm y}$ and the deduced structure is shown in Fig. 4. The primitive tetragonal cell with $P4/mmm$ symmetry contains one formula unit. The position of the oxygen atoms was determined from geometrical considerations and by comparison with related crystal structures. In particular the square-planar coordination of the Cu atoms in the CuO_2 plane between the Ca planes is implied by the short interplanar Cu-Cu distance. The positions of the O atoms in the CuO_5 pyramids were assigned on the basis of a single-crystal determination of the related 2122 structure.[13]

As mentioned earlier, resistivity and Meissner susceptibility data for the 1223 samples exhibit anomalies near 125 and 118 K which are characteristic temperatures of the 2223 phase.[12] One way to explain the high values of Tl relative to Ba and Cu seen by electron microprobe analysis is to assume that there are occasional intergrowths of Tl-O bilayers consistent with local regions of the 2223 phase. Subsequent high-resolution transmission-electron-microscopy studies have indeed found such regions in these samples. Presumably it is these local regions which give rise to the higher-temperature anomalies. This situation is similar to that found in 2223 structure, where bilayer Cu perovskitelike intergrowths in the trilayer structure correlate with a decrease in T_c from 125 to 118 K.[12]

Figures 1 and 2 indicate that sample B has a significantly higher transition temperature than sample A. It was previously noted that microprobe analysis revealed an additional Tl-rich 1223 phase in sample B. In addition to highly localized regions of the 2223 phase, a second intriguing possibility suggested by these data is that Tl can dope the Ca sites. This is compatible with the similar size of the Tl^{3+} and Ca^{2+} ions. Doping of this type would alter the charge-carrier concentration, which is known to strongly affect the superconducting transition temperature in, for example, the $La_{2-x}Sr_x$-$CuO_{4\pm y}$ system.[14] These results suggest a fascinating complexity to the Tl-Ca-Ba-Cu-O family.

In contrast to the 1223 phase the 1021 phase was found to be semiconducting for a wide range of preparative conditions. However, the 1122 compound was superconducting with a transition temperature that varied from 65 to 85 K, depending on the starting composition. As shown in Fig. 4, the 1021, 1122, and 1223 phases
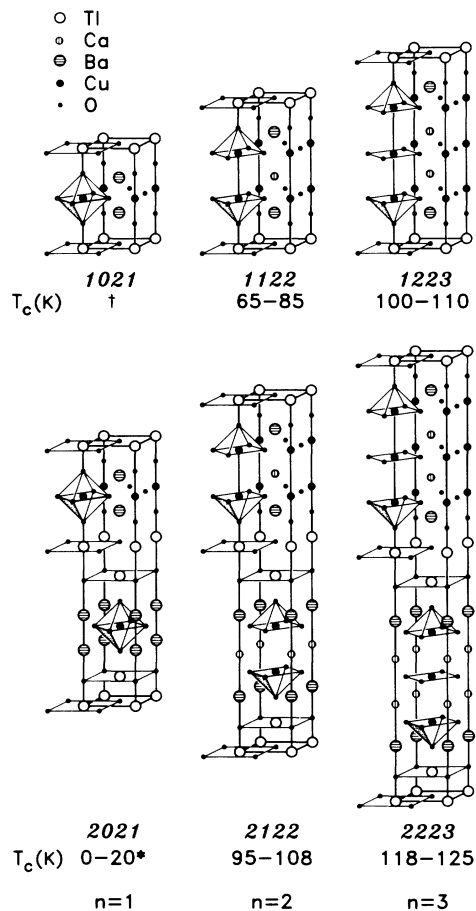
TABLE I. Positional parameters for $Tl_1Ca_2Ba_2Cu_3O_9$, space group D^1_{4h}-$P4/mmm$, $Z=1$, with unit-cell dimensions $a=3.8429(16)$ Å and $c=15.871(3)$ Å. Oxygen atom positions are based on known metal coordination polyhedra in related crystal structures.

Atom	Site	X	Y	Z
Tl	$1a$	0.000	0.000	0.000
Ba	$2h$	0.500	0.500	0.176
Ca	$2h$	0.500	0.500	0.397
Cu(1)	$1b$	0.000	0.000	0.500
Cu(2)	$2g$	0.000	0.000	0.302
O(1)	$2e$	0.000	0.500	0.500
O(2)	$4i$	0.000	0.500	0.304
O(3)	$2g$	0.000	0.000	0.132
O(4)	$1c$	0.500	0.500	0.000

FIG. 4. Unit cells of the $Tl_1Ca_{n-1}Ba_2Cu_nO_{2n+3}$ ($n=1$, 2, and 3) compounds containing Tl-O monolayers and comparison with those of the corresponding compounds Tl_2Ca_{n-1}-$Ba_2Cu_nO_{2n+4}$, containing Tl-O bilayers. The range of superconducting transition temperatures found for each compound is included in the figure. Dagger, no superconductivity observed for 1021 samples prepared under a wide range of preparative conditions. Asterisk, other groups have reported $T_c \approx 85$ K for the 2021 phase (Refs. 11 and 13).

form a series of related structures in which the Cu perovskitelike units contain one, two, or three CuO_2 layers separated in all three cases by a single octahedrally coordinated Tl layer. These structures are analogs of the corresponding 2021, 2122, and 2223 phases (see Fig. 4), which contain similar Cu perovskitelike slabs.[12,13] However, in the latter and in all other previously known superconducting structures in the Bi-Ca-Sr-Cu-O and Tl-Ca-Ba-Cu-O systems, the perovskitelike units are separated by staggered Bi-O or Tl-O bilayers (which cause the unit cells to be body centered). Intuitively one might expect from the highly anisotropic superconducting properties of these perovskitelike materials that the reduced spatial separation of the Cu-O slabs in the new structures (by $\simeq 2.3$ Å in 1223 compared to the 2223 structure) would lead to an enhanced superconducting transition temperature. However, the transition temperature is actually reduced by about $\simeq 15$ and 30 K, respectively, when the Tl-O bilayer is replaced by a Tl-O monolayer for the double and triple CuO_2 layer compounds. The coupling between layers depends on the degree of hybridization of the Tl-O and Cu-O bands. Conceivably this could be greater because of better band overlap in the monolayer case, leading to a reduced $N(E_F)$ and thus lower T_c. Band-structure calculations are in progress to test this possibility.[15]

In conclusion, we have identified a new class of crystal structures, $Tl_1Ca_{n-1}Ba_2Cu_nO_x$ ($x = \simeq 2n + 3$), which unlike all previously known structures in the Tl-Ca-Ba-Cu-O system, contain monolayer Tl-O units which separate a Cu perovskitelike unit. The Cu perovskitelike unit is comprised of one, two, or three CuO_2 layers. As for the bilayer Tl-O analogs, the transition temperatures of these compounds increase with the number of CuO_2 layers in the Cu perovskitelike unit. However, the transition temperatures are lower in each case than those of the corresponding bilayer Tl-O compounds. These structures provide important clues to an improved understanding of the role played by the interlayers that separate the Cu perovskitelike units.

[1]C. Michel, M. Hervieu, M. M. Borel, A. Grandin, F. Deslandes, J. Provost, and B. Raveau, Z. Phys. B **68**, 421 (1987).

[2]M. Maeda, Y. Tanaka, M. Fukutomi, and T. Asano, Jpn. J. Appl. Phys. Pt. 2 **27**, L209 (1988).

[3]R. M. Hazen, C. T. Prewitt, R. J. Angel, N. L. Ross, L. W. Finger, C. G. Hadidiacos, D. R. Veblen, P. J. Heaney, P. H. Hor, R. L. Meng, Y. Y. Sun, Y. Q. Wang, Y. Y. Xue, Z. J. Huang, L. Gao, J. Bechtold, and C. W. Chu, Phys. Rev. Lett. **60**, 1174 (1988).

[4]T. M. Shaw, S. A. Shivanshanker, S. J. LaPlaca, J. J. Cuomo, T. R. McGuire, R. A. Roy, K. H. Kelleher, and D. S. Yee, Phys. Rev. B **37**, 9856 (1988).

[5]D. R. Veblen, P. J. Heaney, R. J. Angel, L. W. Finger, R. M. Hazen, C. T. Prewitt, N. L. Ross, C. W. Chu, P. H. Hor, and R. L. Meng, Nature (London) **332**, 334 (1988).

[6]S. S. P. Parkin, E. M. Engler, V. Y. Lee, A. I. Nazzal, Y. Tokura, J. B. Torrance, and P. M. Grant, Phys. Rev. B (to be published).

[7]J. B. Torrance, Y. Tokura, S. J. LaPlaca, T. C. Huang, R. J. Savoy, and A. I. Nazzal, Solid State Commun. **66**, 703 (1988).

[8]J. M. Tarascon, Y. Le Page, P. Barboux, B. G. Bagley, L. H. Greene, W. R. McKinnon, G. W. Hull, M. Giroud, and D. M. Hwang, Phys. Rev. B **37**, 9382 (1988).

[9]S. A. Sunshine, T. Siegrist, L. F. Schneemeyer, D. W. Murphy, R. J. Cava, B. Batlogg, R. B. van Dover, R. M. Fleming, S. H. Glarum, S. Nakahara, R. Farrow, J. J. Krajewski, S. M. Zahurak, J. V. Waszczak, J. H. Marshall, P. Marsh, L. W. Rupp, and W. F. Peck, Phys. Rev. B **38**, 893 (1988).

[10]Z. Z. Sheng and A. M. Hermann, Nature (London) **332**, 138 (1988).

[11]R. M. Hazen, L. W. Finger, R. J. Angel, C. T. Prewitt, N. L. Ross, C. G. Hadidiacos, P. J. Heaney, D. R. Veblen, Z. Z. Sheng, A. El Ali, and A. M. Hermann, Phys. Rev. Lett. **60**, 1657 (1988).

[12]S. S. P. Parkin, V. Y. Lee, E. M. Engler, A. I. Nazzal, T. C. Huang, G. Gorman, R. Savoy, and R. Beyers, Phys. Rev. Lett. **60**, 2539 (1988).

[13]C. C. Torardi, M. A. Subramanian, J. C. Calabrese, J. Gopalakrishnan, E. M. McCarron, K. J. Morrissey, T. R. Askew, R. B. Flippen, U. Chowdry, and A. W. Sleight, Science **240**, 631 (1988).

[14]M. W. Shafer, T. Penney, and B. L. Olson, Phys. Rev. B **36**, 4047 (1987).

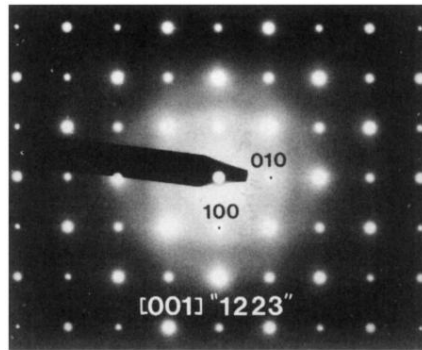[15]F. Herman, R. V. Kasowski, S. J. LaPlaca, and S. S. P. Parkin, unpublished.

FIG. 3. Selected-area transmission-electron-microscopy diffraction pattern along the [001] axis that confirms the primitive tetragonal cell and also indicates the presence of a weak superlattice.
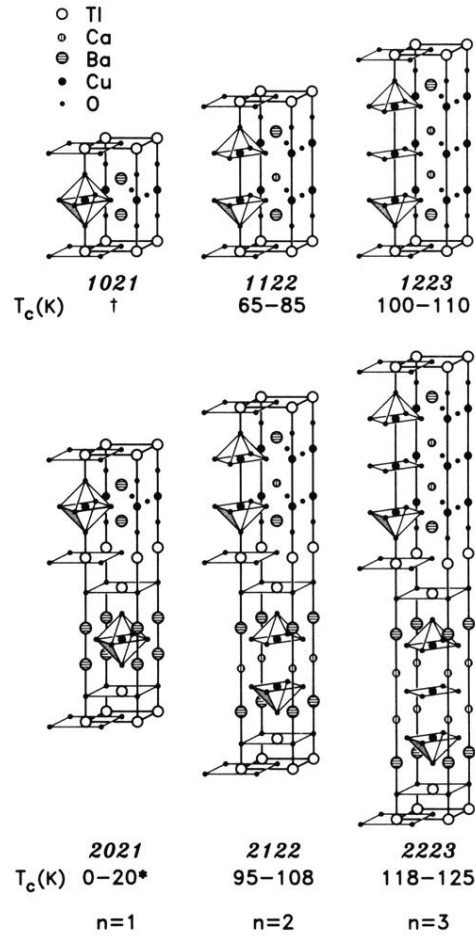
FIG. 4. Unit cells of the $Tl_1Ca_{n-1}Ba_2Cu_nO_{2n+3}$ ($n = 1$, 2, and 3) compounds containing Tl-O monolayers and comparison with those of the corresponding compounds Tl_2Ca_{n-1}-$Ba_2Cu_nO_{2n+4}$, containing Tl-O bilayers. The range of superconducting transition temperatures found for each compound is included in the figure. Dagger, no superconductivity observed for 1021 samples prepared under a wide range of preparative conditions. Asterisk, other groups have reported $T_c \simeq 85$ K for the 2021 phase (Refs. 11 and 13).